

Disordered flat bands on the kagome lattice

Thomas Bilitewski¹ and Roderich Moessner¹

¹Max-Planck-Institut für Physik komplexer Systeme, Nöthnitzer Str. 38, 01187 Dresden, Germany

We study two models of correlated bond- and site-disorder on the kagome lattice considering both translationally invariant and completely disordered systems. The models are shown to exhibit a perfectly flat ground state band in the presence of disorder for which we provide exact analytic solutions. Whereas in one model the flat band remains gapped and touches the dispersive band, the other model has a finite gap, demonstrating that the band touching is not protected by topology alone. Our model also displays fully saturated ferromagnetic groundstates in the presence of repulsive interactions, an example of disordered flat band ferromagnetism.

I. INTRODUCTION

The physics of flat bands has generated considerable excitement over the years^{1–3}. In a flat band, the kinetic energy is completely suppressed; thus, transport is hindered by a vanishing group velocity, and any kind of interaction is non-perturbative in nature and can mix the extensive number of degenerate states in the flat band, with the potential to create complex many-body states and phenomena. One well known example of this mechanism at work is the fractional quantum Hall effect, where interactions induce highly non-trivial behaviour of the electrons in the degenerate Landau levels of a magnetic field.

Thus, flat band systems are well-suited for producing unconventional phenomena^{2,4,5}. For both fermions and bosons, they allow to realise the fractional quantum hall effect in absence of a magnetic field^{6–9}, i.e. fractional Chern Insulators, and at potentially high temperatures¹⁰. Other contexts include high-temperature superconductivity^{11,12}, Wigner crystallisation^{13,14}, realising higher-spin analogs of Weyl-fermions¹⁵, bands with chiral character¹⁶, lattice supersolids¹⁷, fractal geometries¹⁸, magnets with dipolar-interactions¹⁹, and Floquet physics^{20,21}. Flat bands of magnons also play a crucial role in determining the behaviour of quantum magnets in magnetic fields^{22–25}.

Interest in flat band physics is not restricted to the presence of interactions, but also extends to their response to disorder, as the flat band states can turn out to be critical displaying multifractality²⁶, or unconventional localisation behaviour^{27–29}. They also appear in purely classical mechanical systems³⁰, and in the field of photonics^{31,32}. Quite recently, flat bands have been experimentally demonstrated in a realistic Kagome material³³ as well as in optical lattices³⁴.

In this work consider non-interacting nearest neighbour hopping models on the Kagome lattice with correlated bond- and site-disorder, as illustrated in Fig. 1. The simple nearest neighbour hopping model on the Kagome lattice is known to host a degenerate flat band^{35–39} with a quadratic band touching point believed to be topologically protected⁴⁰. However, in interacting many-body physics it is often preferable to work with a gapped flat band to protect it from ‘Landau-level mixing’, i.e. from

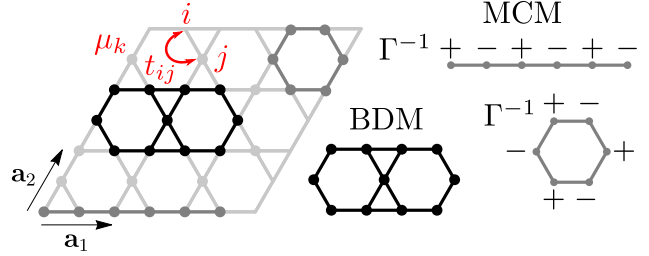


FIG. 1. Kagome lattice with lattice vectors a_1 and a_2 , shown is a finite-size lattice with $L_x = L_y = 3$, opposite edges are identified for periodic boundary conditions. The model contains site-dependent nearest-neighbour tunnelings t_{ij} and chemical potentials μ_k . The highlighted sites correspond to a zero-energy flat band-state of the MCM, hexagon and system-spanning loop (dark gray) or the BDM, double hexagon (black).

interactions with the dispersive bands.

Here, we explicitly construct a gapped flat band on the Kagome lattice. The simplest setting in which it appears contains modulated bond and site-disorder, both in presence of translational symmetry (where one can speak of a band) and in absence of it, i.e. in the presence of random disorder, where one may still identify an extensive manifold of degenerate states. In fact, we find that a local perturbation to the Hamiltonian can open a gap above the flat band. This indicates that the band-touching is protected not just by topology but requires also symmetry.

We obtain exact solutions for the flat band states of all of these models, facilitating a clear interpretation of why the chosen type of correlated site-bond-disorder does not lift the extensive degeneracy of the flat band, and providing new insight into the stability of the flat bands and the protection of the quadratic band-touching point. Our study also adds an example where compactly localised Wannier-states can be explicitly constructed for a disordered flat band model.

Our treatment extends previous observations on the flat band in kagome, such as the observed stability of the flat band and band-touching points to breathing anisotropy⁴¹, and opens up new perspectives: We show how to selectively gap out the flat band, or the Dirac cones, or all bands. Thus, our results reinforces the role

of the kagome lattice as a platform for the study of topological physics and flat band physics in general, in particular the physics of perturbations and disorder in flat bands.

II. MODEL

We study non-interacting particles on the kagome lattice

$$\mathcal{H} = \sum_{\langle i,j \rangle} \left(t_{ij} \hat{c}_i^\dagger \hat{c}_j + c.c. \right) + \sum_i \mu_i \hat{n}_i, \quad (1)$$

with nearest-neighbour (complex) hoppings t_{ij} between sites i, j and site-dependent chemical potentials μ_i at site i . In the models we consider μ_i is given as a function of the couplings t_{ij} . The specific correlation between the hopping and potential terms is motivated by a connection to bond-disordered Heisenberg models⁴² where it naturally arises via an exact rewriting of the Hamiltonian.

The Hamiltonian can be compactly written via its matrix elements H_{ij} as $\mathcal{H} = \sum_{ij} c_i^\dagger H_{ij} c_j$. Noting that this only connects nearest neighbours, and that every nearest neighbour pair belongs either to an up or down triangle of the Kagome lattice, we rewrite the Hamiltonian in the following way

$$\mathcal{H} = \mathcal{H}^\Delta + \mathcal{H}^\nabla \quad (2)$$

$$H_{ij}^{\Delta/\nabla} = \begin{cases} \bar{\gamma}_i^{\Delta/\nabla} \gamma_j^{\Delta/\nabla} + |\gamma_i^{\Delta/\nabla}|^2 \delta_{ij}, & \text{for } i, j \in \alpha \\ 0, & \text{otherwise} \end{cases} \quad (3)$$

where we first split it into its contribution on the up and down triangles, and then define all couplings within a triangle α via site and triangle dependent (complex) factors $\gamma_i^{\Delta/\nabla}$.

This form makes the correlation between the hoppings and chemical potentials explicit. Specifically, we have $t_{ij} = \bar{\gamma}_i^\alpha \gamma_j^\alpha$ for sites i, j in the triangle α and $\mu_i = |\gamma_i^\Delta|^2 + |\gamma_i^\nabla|^2$. In the presence of lattice-inversion symmetry $\mathcal{H}^\Delta = \mathcal{H}^\nabla$ and these factors become solely site-dependent. We will refer to the model with lattice inversion symmetry as the maximal Coulomb model (MCM), and with broken lattice inversion symmetry as the bond-disordered model (BDM).

This also allows us to make an insightful connection to the Hamiltonian of the non-disordered model, essentially the disordered model can be understood as a rescaling of the clean model by the γ factors. Using that the Hamiltonian is fully specified by its matrix elements H_{ij} , we can further split them as a product of three matrices as

$$H^{\Delta/\nabla} = \bar{\Gamma}^{\Delta/\nabla} H_0^{\Delta/\nabla} \Gamma^{\Delta/\nabla} \quad (4)$$

with $\Gamma_{ij}^{\Delta/\nabla} = \delta_{ij} \gamma_i^{\Delta/\nabla}$, a diagonal matrix containing the scaling factors, and H_0 the matrix of the clean system with $\gamma_i^\alpha \equiv 1$, describing the nearest neighbour hopping on the kagome lattice.

Making use of the form $\mathcal{H} = \sum_{ij} c_i^\dagger H_{ij} c_j$ the action of the Hamiltonian on single particle states $|\Psi\rangle = \sum_i \psi_i c_i^\dagger |\text{vac}\rangle$ is simply

$$\mathcal{H}|\Psi\rangle = \sum_i H_{ik} \psi_k c_i^\dagger |\text{vac}\rangle = \sum_i (H\psi)_i c_i^\dagger |\text{vac}\rangle. \quad (5)$$

From this we obtain the expectation value as

$$\langle \Psi | \mathcal{H} | \Psi \rangle = \sum_{ij} \bar{\psi}_i H_{ij} \psi_j = \sum_\alpha \left| \sum_{i \in \alpha} \gamma_i^\alpha \psi_i \right|^2 = \sum_\alpha |\psi_\alpha|^2, \quad (6)$$

where in the second equality we used the explicit form of the Hamiltonian, Eq. 3, which splits into a sum over triangles α , and in the last equality defined the sum of scaled amplitudes within a triangle $\psi_\alpha = \sum_{i \in \alpha} \gamma_i^\alpha \psi_i$.

Thus, exact zero-modes are states with $\psi_\alpha = 0$ on all triangles α . This condition is typically referred to as a groundstate constraint in the theory of frustrated magnets and is intimately connected to height-mappings and emergent gauge theory descriptions of the groundstate phase. For spins the condition $\psi_\alpha = 0$ is more stringent and can only be fulfilled for not too disparate bond values due to the unit length constraint which is found to lead to a phase transition of the model. In contrast, here it can be fulfilled for arbitrary choices.

III. CONSTRUCTION OF FLAT BAND STATES

Exact Mapping of flat band for the MCM: The clean system is known to host an exactly flat band at $E = 0$ which touches the dispersive band at $q = 0$ ⁴⁰.

In the non-disordered model ($\gamma_i^\alpha = 1$), the ground state condition $\psi_\alpha = \sum_{i \in \alpha} \psi_i = 0$ reduces to the simple sum of amplitudes in every triangle vanishing. It is easy to check that the states illustrated in Fig. 1, a hexagon loop with alternating $+, -$, and a system-spanning loop with alternating $+, -$ amplitudes, satisfy this, and (less-trivially) that these yield $N_s/3+1$ linearly independent zero-energy states. Since the kagome lattice has 3 sites in the unit cell and thus 3 bands, finding $N_s/3+1$ states at the same energy then also implies the band-touching.

For the MCM all these zero-modes of the clean system can be mapped to zero-modes of the disordered model via

$$\Psi_{\text{MCM}}^{\text{FB}} = \Gamma^{-1} \Psi_0^{\text{FB}}, \quad (7)$$

which follows directly from $H^\Delta = H^\nabla$ in the MCM together with Eq. 4 and Eq. 5, e.g. the observation that the disordered model can be understood as a rescaling of the clean model. Thus, we obtain an exactly flat band at $E = 0$. This further implies that the band touching point is preserved as well.

The flat band states of the MCM can therefore be characterised the same way as in the clean system⁴⁰: The MCM (a) $N_s/3+1$ zero-modes, (b) of which $(N_s/3-1)$

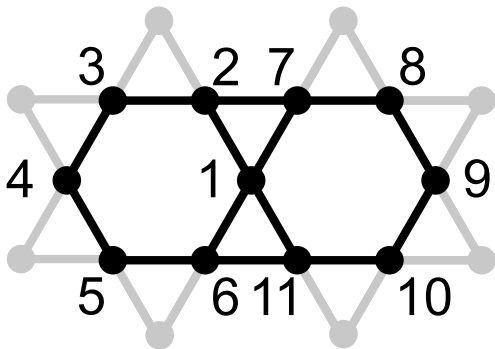


FIG. 2. A double hexagon of the kagome lattice. The wavefunction of a BDM zero energy state is localised on the black sites. Note that the state occupies 11 sites, and is part of 10 triangles, thus, there are 11 degrees of freedom and 10 constraints, in addition to the wavefunction normalisation, implying that there is a unique solution for such a localised state.

can be chosen as lin. independent localised hexagon loop modes and 2 as system-spanning delocalised loops (both types arising via the mapping from the zero-modes of the clean system), and (c) the flat band is gapless touching the dispersive band. The two different types of states are schematically illustrated in Fig. 1.

We emphasise that this is completely independent of the specifics of γ_i , e.g. it holds true for translationally invariant, completely disordered, positive, negative and sign-changing, and real or complex choices. In fact, it holds true for a slightly more general model, where $\Gamma^\Delta = c\Gamma^\nabla$ which in particular includes the model with breathing anisotropy.

Construction of flat band for BDM: We note that such a mapping is not possible for the BDM where Γ differs non-trivially between up- and down-triangles. Thus, it is not immediately obvious that the BDM should host an extensively degenerate groundstate band and if so whether the band-touching point is preserved.

We first summarise the findings and then provide a construction of the flat band states. We find that (a) the BDM has $N_s/3$ exact zero-modes/flat band, (b) the flat band states can all be localised and (c) the flat band is generically gapped.

We emphasise the last point, stating that it is possible to maintain the flatness of the band while gapping it from the dispersive bands in contrast to the claimed topological protection⁴⁰. We will analytically show this in the next section for translationally invariant model, and provide numerical evidence for disordered systems. In fact, it is sufficient to break inversion symmetry by changing a single coupling γ_i^Δ to create a gap to the flat band.

We now explicitly construct the $N_s/3$ linearly independent localised states forming the degenerate flat band. To do so, we consider a double hexagon of the kagome lattice

shown with our conventions for the site labels in Fig. 2. We note that such a state occupies 11 sites and these sites are part of 10 triangles of the kagome lattice. Each triangle contributes one scalar constraint $\Psi_\alpha = 0$, in addition to one normalisation constraint, thus, we might expect a unique solution on every hexagon-pair.

The resulting linear system of equations can be solved explicitly (see SM⁴³), and the wave-function amplitudes may be written as a function of the coupling terms γ_i^α as $\Psi_i = \Psi_1 f_i(\gamma_i^\alpha)/D(\gamma_i^\alpha)$. This solution is only valid if the determinant D given by

$$\Delta = \gamma_3^\nabla \gamma_5^\nabla \gamma_7^\nabla \gamma_9^\nabla \gamma_{11}^\nabla \gamma_2^\Delta \gamma_4^\Delta \gamma_6^\Delta \gamma_8^\Delta \gamma_{10}^\Delta - (\nabla \leftrightarrow \Delta), \quad (8)$$

is non-zero. This manifestly vanishes in the presence of inversion symmetry ($\gamma^\Delta = \gamma^\nabla$), but is non-zero if inversion symmetry is broken ($\gamma^\Delta \neq \gamma^\nabla$). Therefore, in the BDM there is a unique localised state on every double-hexagon.

We have checked (numerically) that taking L^2 such double-hexagons tiling the full kagome lattice does yield L^2 independent states, thus, providing a full basis for the zero-energy states of the BDM, in contrast to the MCM and the clean system which requires the system spanning loop states⁴⁰.

It is also easy to show that no such solution for a localised state is possible on a single hexagon (see SM⁴³), thus, proving that these found states indeed form a maximally localised basis of the flat band manifold.

Typically, in presence of interactions the size of the maximally localised basis states strongly affects the behaviour of the model, and here we find that this size doubles in presence of infinitesimal disorder. In fact, the existence of a compactly localised basis for flat bands is an open question of research with relations to the topology of the corresponding Bloch bands^{44–46}.

IV. GAPPED FLAT BANDS

It remains to show that the BDM flat band states are indeed gapped and do not touch the dispersive bands, which we will show in the next sections both for translationally invariant and generic disordered models.

Translationally invariant systems: We begin by considering translationally invariant systems with real couplings. In that case the model has 6 (3) free parameters $\gamma_{A,B,C}^{\Delta/\nabla}$ for BDM (MCM), e.g. the couplings on the three sites (A,B,C) in a triangle of the Kagome lattice, with different couplings on the up and down triangle for the BDM model.

In this case, one can analyse the model in momentum space, and analytical results can be obtained (see SM⁴³). We find that for every q there is exactly one zero-mode, i.e. we find a flat band at $E = 0$ for both the BDM and MCM as anticipated from the construction of the zero-modes above. Importantly, this allows us to obtain an analytic expression for the gap of the BDM, thus,

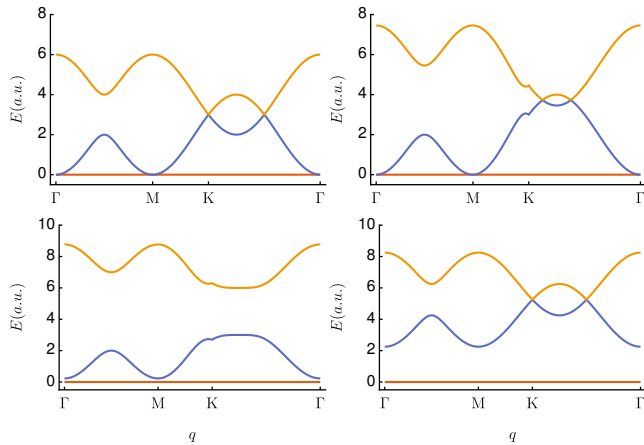


FIG. 3. Dispersion along high-symmetry lines in the Brillouin zone. From top left to bottom right: clean system, MCM with $\gamma_A = \gamma_A^\Delta = \gamma_A^\nabla < \sqrt{2}$, BDM with $\gamma_A = 2$ and BDM with $\gamma_A^\Delta = \frac{1}{\gamma_A^\nabla} = \gamma_B^\nabla = \frac{1}{\gamma_B^\Delta} = 0.5$.

proving our claim that the BDM flat band can indeed be gapped.

We will consider illustrative examples for the gap below, please see SM⁴³ for the general expression of the gap. As the simplest model consider just $\gamma_A^\Delta \neq 1$, then the gap scales as

$$\Delta_{\text{gap}} = \frac{1}{2} \left(5 + \gamma_A^{\Delta 2} - \sqrt{(\gamma_A^{\Delta 2} + 1)^2 + 16\gamma_A^\Delta + 16} \right) \quad (9)$$

showing a quadratic scaling for small deviations away from the homogeneous system.

A more symmetric arrangement can be obtained by considering $\gamma_A^\Delta = \frac{1}{\gamma_A^\nabla} = \gamma_B^\nabla = \frac{1}{\gamma_B^\Delta} = x$, which yields the gap to the flat band as

$$\Delta_{\text{gap}} = x^2 + x^{-2} - 2. \quad (10)$$

We note that this allows to cleanly separate the flat band by an (arbitrarily) large gap from all dispersive bands, making the Kagome lattice a prime platform to study physics in flat bands.

We show dispersion relations along high-symmetry lines in the Brillouin zone for the clean model, the MCM and the BDM in Fig. 3. We emphasise that clearly both models retain an exactly flat band at $E = 0$. As discussed above the MCM always retains the band-touching point at $q = 0$ (Γ point), but the Dirac-points can be gapped for large perturbations (not shown).

In contrast in the BDM, the flat band is always gapped as seen in the lower panel of Fig. 3, already for infinitesimal changes in the couplings. Just changing a single coupling generically gaps both the flat band and the Dirac points (lower left panel). For the symmetric choice described above, the flat band is gapped, but the Dirac points remain gapless (lower right panel).

In summary, we have shown that we can selectively gap out the flat bands and keep the Dirac cones or gap out

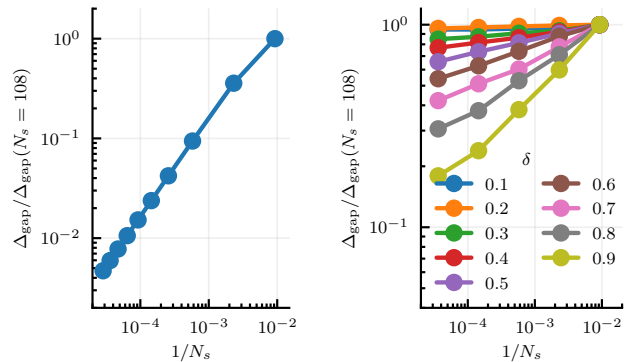


FIG. 4. (a) Gap of the flat band in presence of a local perturbation versus inverse number of sites N_s on a log-log scale showing a linear scaling with inverse number of sites $\sim N_s^{-1}$. (b) Gap of the flat band for the fully disordered system versus inverse number of sites for different disorder strengths δ .

the Dirac cones, but keep the quadratic band touching point, or gap out all bands.

Local Perturbation: Before considering fully disordered models it is insightful to understand the effect of a local perturbation to the system. For a topologically protected band-crossing one would expect the resulting gap to scale to zero exponentially in system size.

We modify the Hamiltonian locally by changing a single coupling γ^Δ affecting one site potential μ and two tunnel couplings t . As a result, in Fig. 4(a) we observe a linear decrease of the gap with inverse number of sites $\sim N_s^{-1}$, consistent with the gap closing in the thermodynamic limit. However, the decay is clearly not exponential as would be expected for a topologically protected degeneracy.

Disordered Systems: Next, we consider fully disordered models with random choices for $\gamma_i^{\Delta/\nabla}$. As an example we consider a box-uniform distribution $\gamma \in [1 - \delta, 1 + \delta]$. However, we emphasise that this specific choice is not relevant and the conclusions hold true for any generic disorder distribution.

The gap to the flat band versus inverse system size for a range of values of δ is shown in Fig. 4(b). It extrapolates to a finite value in the thermodynamic limit for $\delta < 1$, and scales as δ^2 for small disorder strengths. Thus, we conclude that disorder of this type gaps out the flat band, even for infinitesimal disorder strength.

We also note in passing that the finite gap implies that the projector into the flat band decays exponentially for the BDM model, but decays algebraically for the gapless MCM.

Flat Band Ferromagnetism in a disordered model: Flat bands are known to host ferromagnetic phases in presence of repulsive interactions^{35–39,47}. The presence of a gap to the flat band in our model ensures that the many-body groundstate at filling $n = 1/6$ is the unique fully-saturated ferromagnetic state.

To see this in our model of disordered flat bands, we

consider a fermionic version with repulsive Hubbard interactions,

$$\mathcal{H} = \sum_{\langle i,j \rangle, \sigma} \left(t_{ij} \hat{c}_{i\sigma}^\dagger \hat{c}_{j\sigma} + c.c. \right) + \sum_i \mu_i \hat{n}_i + U \sum_i n_{\uparrow} n_{\downarrow}, \quad (11)$$

for spin 1/2 fermions, $n_i = n_{i\uparrow} + n_{i\downarrow}$, t_{ij} and μ_i are chosen as above, and we consider the BDM to have a flat gapped non-interacting band.

Since for $U > 0$ the interaction term is positive, and the kinetic energy is positive-definite by construction, many body states with $E = 0$ are necessarily groundstates.

One groundstate is easily obtained by filling the non-interacting flat band completely with polarised spins which do not interact. Thus, we have at filling $n = 1/6$ a ferromagnetic groundstate with maximal spin $S = L^2/2$, with the full $2S(2S + 1)$ degeneracy due to the $SU(2)$ symmetry of the model. The main question to obtain ferromagnetism is whether this groundstate is unique, or if there are additional non-magnetic states as well. Here, it turns out that the groundstate is gapped, since the non-interacting band-structure has a finite gap for the BDM.

We performed exact diagonalisation of the Hubbard model, Eq. 11, on small finite-size Kagome clusters (2×2 , 2×3) to confirm that the groundstate is indeed of the described form.

Finally, due to the presence of a spectral gap, we expect the ferromagnetism to be stable to finite perturbations and fluctuations in the particle number. Indeed, ferromagnetism is expected to be enhanced compared to the usual Kagome case, since the localised non-interacting states now contain two hexagons.

V. OUTLOOK

Demonstrating that the flat bands of the kagome lattice can be gapped opens up the kagome lattice as a prime platform for the clean, i.e. isolated from the dispersive bands by an arbitrarily large gap, study of topological and more general flat band phenomena.

In addition, the presence of a flat band in a disordered model is highly non-trivial and of general interest even if it requires fine-tuning between the hopping and site-potential terms.

In terms of realisations of the specific type of couplings: We recall that this model is naturally realised in the large-N limit^{48,49} of a classical nearest-neighbour bond-disordered Heisenberg-(Anti)ferromagnet, where the correlation between site- and bond-disorder arises from the spin length constraint. In other settings it is unlikely that bond- and site-disorder is correlated in the required way, thus, the system would need to be specifically designed. In this case we envision it would be considerably easier to realise the translationally invariant model reducing the required number of parameters that have to be tuned. (For the minimal model we would require tuning 1 site-potential and 2 tunneling couplings in each unit cell). This might be feasible in cold-gas setups where control over individual sites and bonds is possible by the use of quantum gas microscopes.

In terms of topological properties of the flat band, we note that fluxes in the MCM model are trivial by construction (since they can be removed by a unitary gauge transformation). The BDM model in contrast supports non-trivial fluxes along the hexagon loops of the lattice. However, since in the BDM model all states of the flat band can be chosen localised, the non-interacting model is necessarily topologically trivial⁵⁰.

Our model also presents a natural realisation of flat band ferromagnetism on the Kagome lattice, where the gap of the single particle spectrum results in a unique gapped fully saturated ferromagnetic many-body state in presence of repulsive on-site interactions. We reserve the further discussion of interacting many-body phases in the gapped flat band and the effects on the magnon bands of magnets for future work.

It might also be interesting to explore the effect of longer-range interactions on the flat bands of this model which have recently been found to be remarkably stable for the non-disordered model¹⁹.

Acknowledgements: We thank J. Richter for insightful discussions and comments on a first draft of this paper. This work was in part supported by Deutsche Forschungsgemeinschaft via SFB 1143.

¹ H. Tasaki, “From Nagaoka’s Ferromagnetism to Flat-Band Ferromagnetism and Beyond: An Introduction to Ferromagnetism in the Hubbard Model,” *Progress of Theoretical Physics* **99**, 489–548 (1998).

² Oleg Derzhko, Johannes Richter, and Mykola Maksymenko, “Strongly Correlated Flat-band Systems: The Route from Heisenberg Spins to Hubbard Electrons,” *International Journal of Modern Physics B* **29**, 1530007 (2015).

³ Daniel Leykam, Alexei Andreanov, and Sergej Flach, “Artificial flat band systems: from lattice models to experi-

ments,” *Advances in Physics: X* **3**, 1473052 (2018).

⁴ Siddharth A. Parameswaran, Rahul Roy, and Shivaji L. Sondhi, “Fractional Quantum Hall Physics in Topological Flat Bands,” *C. R. Phys.* **14**, 816–839 (2013).

⁵ Emil J. Bergholtz and Zhao Liu, “Topological Flat Band Models and Fractional Chern Insulators,” *International Journal of Modern Physics B* **27**, 1330017 (2013).

⁶ D.N. Sheng, Zheng-Cheng Gu, Kai Sun, and L. Sheng, “Fractional quantum hall effect in the absence of Landau levels,” *Nature Communications* **2**, 389 (2011).

⁷ Yi-Fei Wang, Zheng-Cheng Gu, Chang-De Gong, and

- D. N. Sheng, “Fractional Quantum Hall Effect of Hard-Core Bosons in Topological Flat Bands,” *Phys. Rev. Lett.* **107**, 146803 (2011).
- ⁸ Titus Neupert, Luiz Santos, Claudio Chamon, and Christopher Mudry, “Fractional Quantum Hall States at Zero Magnetic Field,” *Phys. Rev. Lett.* **106**, 236804 (2011).
- ⁹ Kai Sun, Zhengcheng Gu, Hosho Katsura, and S. Das Sarma, “Nearly Flatbands with Nontrivial Topology,” *Phys. Rev. Lett.* **106**, 236803 (2011).
- ¹⁰ Evelyn Tang, Jia-Wei Mei, and Xiao-Gang Wen, “High-temperature fractional quantum hall states,” *Phys. Rev. Lett.* **106**, 236802 (2011).
- ¹¹ Masatoshi Imada and Masanori Kohno, “Superconductivity from flat dispersion designed in doped mott insulators,” *Phys. Rev. Lett.* **84**, 143–146 (2000).
- ¹² Sebastiano Peotta and Päivi Törmä, “Superfluidity in topologically nontrivial flat bands,” *Nature Communications* **6**, 8944 (2015).
- ¹³ Congjun Wu, Doron Bergman, Leon Balents, and S. Das Sarma, “Flat bands and wigner crystallization in the honeycomb optical lattice,” *Phys. Rev. Lett.* **99**, 070401 (2007).
- ¹⁴ Błażej Jaworowski, Alev Devrim Gçl, Piotr Kaczmarkiewicz, Michał Kupczyński, Paweł Potasz, and Arkadiusz Wójs, “Wigner crystallization in topological flat bands,” *New Journal of Physics* **20**, 063023 (2018).
- ¹⁵ Balázs Dóra, Janik Kailasvuori, and R. Moessner, “Lattice generalization of the Dirac equation to general spin and the role of the flat band,” *Phys. Rev. B* **84**, 195422 (2011).
- ¹⁶ Ajith Ramachandran, Alexei Andreanov, and Sergej Flach, “Chiral flat bands: Existence, engineering, and stability,” *Phys. Rev. B* **96**, 161104 (2017).
- ¹⁷ Sebastian D. Huber and Ehud Altman, “Bose condensation in flat bands,” *Phys. Rev. B* **82**, 184502 (2010).
- ¹⁸ Biplab Pal and Kush Saha, “Flat bands in fractal-like geometry,” *Phys. Rev. B* **97**, 195101 (2018).
- ¹⁹ Mykola Maksymenko, Roderich Moessner, and Kirill Shtengel, “Persistence of the flat band in a kagome magnet with dipolar interactions,” *Phys. Rev. B* **96**, 134411 (2017).
- ²⁰ Liang Du, Xiaoting Zhou, and Gregory A. Fiete, “Quadratic band touching points and flat bands in two-dimensional topological Floquet systems,” *Phys. Rev. B* **95**, 035136 (2017).
- ²¹ Pedro Roman-Taboada and Gerardo G. Naumis, “Topological flat bands in time-periodically driven uniaxial strained graphene nanoribbons,” *Phys. Rev. B* **95**, 115440 (2017).
- ²² J. Schulenburg, A. Honecker, J. Schnack, J. Richter, and H.-J. Schmidt, “Macroscopic Magnetization Jumps due to Independent Magnons in Frustrated Quantum Spin Lattices,” *Phys. Rev. Lett.* **88**, 167207 (2002).
- ²³ M. E. Zhitomirsky and Hirokazu Tsunetsugu, “High Field Properties of Geometrically Frustrated Magnets,” *Progress of Theoretical Physics Supplement* **160**, 361–382 (2005).
- ²⁴ Heinz-Jürgen Schmidt, Johannes Richter, and Roderich Moessner, “Linear Independence of Localized Magnon States,” *J. Phys. A: Math. Gen.* **39**, 10673 (2006).
- ²⁵ O. Derzhko, J. Richter, A. Honecker, and H.-J. Schmidt, “Universal Properties of Highly Frustrated Quantum Magnets in Strong Magnetic Fields,” *Low Temp. Phys.* **33**, 745–756 (2007).
- ²⁶ J. T. Chalker, T. S. Pickles, and Pragya Shukla, “Anderson localization in tight-binding models with flat bands,” *Phys. Rev. B* **82**, 104209 (2010).
- ²⁷ Sergej Flach, Daniel Leykam, Joshua D. Bodyfelt, Peter Matthies, and Anton S. Desyatnikov, “Detangling Flat Bands into Fano Lattices,” *EPL (Europhysics Letters)* **105**, 30001 (2014).
- ²⁸ Joshua D. Bodyfelt, Daniel Leykam, Carlo Danieli, Xiaoquan Yu, and Sergej Flach, “Flatbands under correlated perturbations,” *Phys. Rev. Lett.* **113**, 236403 (2014).
- ²⁹ Daniel Leykam, Joshua D. Bodyfelt, Anton S. Desyatnikov, and Sergej Flach, “Localization of weakly disordered flat band states,” *The European Physical Journal B* **90**, 1 (2017).
- ³⁰ Nathan Perchikov and O. V. Gendelman, “Flat bands and compactons in mechanical lattices,” *Phys. Rev. E* **96**, 052208 (2017).
- ³¹ Yuanyuan Zong, Shiqiang Xia, Liqin Tang, Daohong Song, Yi Hu, Yumiao Pei, Jing Su, Yigang Li, and Zhigang Chen, “Observation of Localized Flat-band States in Kagome Photonic Lattices,” *Opt. Express* **24**, 8877 (2016).
- ³² Daniel Leykam and Sergej Flach, “Perspective: Photonic flatbands,” *APL Photonics* **3**, 070901 (2018).
- ³³ Zhiyong Lin, Jin-Ho Choi, Qiang Zhang, Wei Qin, Seho Yi, Pengdong Wang, Lin Li, Yifan Wang, Hui Zhang, Zhe Sun, Laiming Wei, Shengbai Zhang, Tengfei Guo, Qingyou Lu, Jun-Hyung Cho, Changgan Zeng, and Zhenyu Zhang, “Flatbands and emergent ferromagnetic ordering in fe_3sn_2 kagome lattices,” *Phys. Rev. Lett.* **121**, 096401 (2018).
- ³⁴ Gyu-Boong Jo, Jennie Guzman, Claire K. Thomas, Pavan Hosur, Ashvin Vishwanath, and Dan M. Stamper-Kurn, “Ultracold atoms in a tunable optical kagome lattice,” *Phys. Rev. Lett.* **108**, 045305 (2012).
- ³⁵ A Mielke, “Ferromagnetic ground states for the hubbard model on line graphs,” *Journal of Physics A: Mathematical and General* **24**, L73 (1991).
- ³⁶ A Mielke, “Ferromagnetism in the hubbard model on line graphs and further considerations,” *Journal of Physics A: Mathematical and General* **24**, 3311 (1991).
- ³⁷ A Mielke, “Exact ground states for the Hubbard model on the Kagome lattice,” *Journal of Physics A: Mathematical and General* **25**, 4335 (1992).
- ³⁸ Hal Tasaki, “Ferromagnetism in the Hubbard models with degenerate single-electron ground states,” *Phys. Rev. Lett.* **69**, 1608–1611 (1992).
- ³⁹ Andreas Mielke and Hal Tasaki, “Ferromagnetism in the Hubbard model. Examples from models with degenerate single-electron ground states,” *Comm. Math. Phys.* **158**, 341–371 (1993).
- ⁴⁰ Doron L. Bergman, Congjun Wu, and Leon Balents, “Band touching from real-space topology in frustrated hopping models,” *Phys. Rev. B* **78**, 125104 (2008).
- ⁴¹ Karim Essafi, L D C Jaubert, and M Udagawa, “Flat Bands and Dirac Cones in Breathing Lattices,” *J. Phys.: Condens. Matter* **29**, 315802 (2017).
- ⁴² Thomas Bilitewski, Mike E. Zhitomirsky, and Roderich Moessner, “Jammed Spin Liquid in the Bond-Disordered Kagome Antiferromagnet,” *Phys. Rev. Lett.* **119**, 247201 (2017).
- ⁴³ See Supplemental Material at [URL will be inserted by publisher] for additional details on the construction of the localised states and the derivation of the gap for translationally invariant models.
- ⁴⁴ Wulayimu Maimaiti, Alexei Andreanov, Hee Chul Park, Oleg Gendelman, and Sergej Flach, “Compact localized states and flat-band generators in one dimension,” *Phys. Rev. B* **95**, 115135 (2017).

- ⁴⁵ W. Maimaiti, S. Flach, and A. Andreanov, “Universal $d = 1$ flatband generator from compact localized states,” (2018), [arXiv:1810.08199](#).
- ⁴⁶ J.-W. Rhim and B.-J. Yang, “Classification of flat bands from irremovable discontinuities of Bloch wave functions,” (2018), [arXiv:1808.05926](#).
- ⁴⁷ Hal Tasaki, “Stability of ferromagnetism in Hubbard models with nearly flat bands,” *Journal of Statistical Physics* **84**, 535–653 (1996).
- ⁴⁸ H. E. Stanley, “Spherical Model As the Limit of Infinite Spin Dimensionality,” *Phys. Rev.* **176**, 718–722 (1968).
- ⁴⁹ D. A. Garanin and Benjamin Canals, “Classical spin liquid: Exact solution for the infinite-component antiferromagnetic model on the kagomé lattice,” *Phys. Rev. B* **59**, 443–456 (1999).
- ⁵⁰ N. Read, “Compactly supported Wannier functions and algebraic K -theory,” *Phys. Rev. B* **95**, 115309 (2017).
- ⁵¹ K. Roychowdhury, D. Zeb Rocklin, and M. J. Lawler, “Spin Origami with Weyl and Dirac Line Nodes in Distorted Kagome Antiferromagnets,” [ArXiv e-prints](#) (2017).

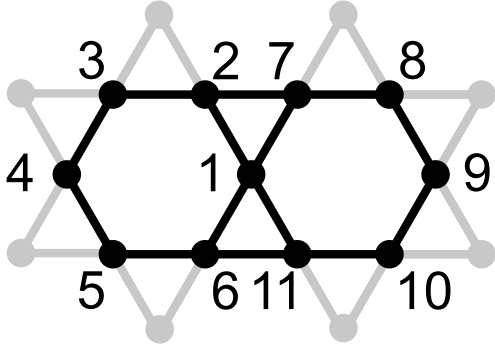


FIG. S1. A double hexagon of the kagome lattice. The wavefunction of a BDM zero energy state is localised on the black sites. Note that the state occupies 11 sites, and is part of 10 triangles, thus, there are 11 degrees of freedom and 10 constraints, in addition to the wavefunction normalisation, implying that there is a unique solution for such a localised state. Same as Fig. 2 in main text, reproduced here to be self-contained.

Supplemental Material:

S1. CONSTRUCTION OF FLAT BAND STATES FOR BDM

In this section we provide additional detail on the explicit construction of the zero-modes of the BDM model. The conventions are illustrated in Fig. S1, same as in main text.

A. Single Hexagon

We begin by showing that for the BDM it is impossible to localise a state on a single hexagon.

An intuitive picture of how states can be localised is as follows: Selecting a subset of sites from the lattice, a necessary condition for a state with amplitudes only on these sites is that the hoppings to sites outside the chosen subset interfere destructively.

For a single hexagon loop, this requires that the tunnelling to all the points of the “star of david” vanishes. Starting at say site 1, this then fixes all the amplitudes of the wavefunction going around the loop step by step. However, after going around the full loop, again arriving at site 1, we require that the amplitude turns out to be the same we started with. This then sets a necessary condition on the values of the couplings for single hexagon localised states to exist.

Starting at say site 1, we require $\gamma_1^\nabla \Psi_1 + \gamma_2^\nabla \Psi_2 = 0$, which we can solve for $\Psi_2 = -\frac{\gamma_1^\nabla}{\gamma_2^\nabla} \Psi_1$, continuing with $\gamma_2^\Delta \Psi_2 + \gamma_3^\Delta \Psi_3 = 0$, which we solve for $\Psi_3 = \frac{\gamma_1^\nabla}{\gamma_2^\nabla} \frac{\gamma_2^\Delta}{\gamma_3^\Delta} \Psi_1$, and similarly along the loop until we again arrive at Ψ_1 .

Writing the final condition out explicitly yields

$$\frac{\gamma_1^\nabla}{\gamma_2^\nabla} \frac{\gamma_2^\Delta}{\gamma_3^\Delta} \frac{\gamma_3^\nabla}{\gamma_4^\nabla} \frac{\gamma_4^\Delta}{\gamma_5^\Delta} \frac{\gamma_5^\nabla}{\gamma_6^\nabla} \frac{\gamma_6^\Delta}{\gamma_1^\Delta} \Psi_1 = \Psi_1, \quad (\text{S1})$$

or by rearrangement

$$\frac{\gamma_1^\Delta}{\gamma_1^\nabla} \frac{\gamma_3^\Delta}{\gamma_3^\nabla} \frac{\gamma_5^\Delta}{\gamma_5^\nabla} = \frac{\gamma_2^\Delta}{\gamma_2^\nabla} \frac{\gamma_4^\Delta}{\gamma_4^\nabla} \frac{\gamma_6^\Delta}{\gamma_6^\nabla} \quad (\text{S2})$$

We note that this condition, in a slightly different notation and context, has been derived previously^{S51}.

Eq. (S2) immediately shows that for the BDM for which $\gamma^\Delta \neq \gamma^\nabla$, e.g. for broken inversion symmetry, single hexagon loops cannot exist. In the presence of inversion symmetry, e.g. for the MCM, this condition is satisfied and states can be localised on a single hexagon as is well known for the clean model.

B. Double Hexagon

Next we consider the double hexagon loop. As for the single hexagon we have some sites on the periphery for which we require destructive interference (8 conditions), in addition we have two internal triangles (2 conditions), for in total 10 conditions for 11 wavefunction amplitudes, which considering the normalisation choice, can uniquely determine the wavefunction if a solution is possible at all.

We have equations of the form

$$\gamma_2^\Delta \Psi_2 + \gamma_3^\Delta \Psi_3 = 0 \quad (\text{periphery}) \quad (\text{S3})$$

$$\gamma_1^\nabla \Psi_1 + \gamma_2^\nabla \Psi_2 + \gamma_7^\nabla \Psi_7 = 0 \quad (\text{internal triangle}) \quad (\text{S4})$$

To determine the solubility of the resulting linear system of equations, one may set $\Psi_1 = 1$ and consider the determinant of the matrix which turns out to be

$$D = \gamma_3^\nabla \gamma_5^\nabla \gamma_7^\nabla \gamma_9^\nabla \gamma_{11}^\nabla \gamma_2^\Delta \gamma_4^\Delta \gamma_6^\Delta \gamma_8^\Delta \gamma_{10}^\Delta - \gamma_3^\Delta \gamma_5^\Delta \gamma_7^\Delta \gamma_9^\Delta \gamma_{11}^\Delta \gamma_2^\nabla \gamma_4^\nabla \gamma_6^\nabla \gamma_8^\nabla \gamma_{10}^\nabla. \quad (\text{S5})$$

In the absence of inversion symmetry ($\gamma^\Delta \neq \gamma^\nabla$), this determinant is generically non-zero, and we obtain a unique solution for the state localised on a double-hexagon.

We also note that in presence of inversion symmetry this determinant vanishes as expected, since then we would have two linearly independent localised states on each hexagon, and any linear combination of them would also form a state localised on the double hexagon.

S2. TRANSLATIONALLY INVARIANT MODELS

In this section we present the explicit expression for the Hamiltonian in momentum space, the flat band eigenstates at generic momentum and the gap at the Γ -point for the BDM model discussed in the main text.

The Hamiltonian in momentum space reads

$$\begin{pmatrix} |\gamma_A^\nabla|^2 + |\gamma_A^\Delta|^2 & \gamma_A^\nabla e^{-i\mathbf{k}\cdot\delta_{AB}} (\gamma_B^\nabla)^* + \gamma_A^\Delta e^{i\mathbf{k}\cdot\delta_{AB}} (\gamma_B^\Delta)^* & \gamma_A^\nabla e^{-i\mathbf{k}\cdot\delta_{AC}} (\gamma_C^\nabla)^* + \gamma_A^\Delta e^{i\mathbf{k}\cdot\delta_{AC}} (\gamma_C^\Delta)^* \\ e^{i\mathbf{k}\cdot\delta_{AB}} \gamma_B^\nabla (\gamma_A^\nabla)^* + e^{-i\mathbf{k}\cdot\delta_{AB}} \gamma_B^\Delta (\gamma_A^\Delta)^* & |\gamma_B^\nabla|^2 + |\gamma_B^\Delta|^2 & \gamma_B^\nabla e^{-i\mathbf{k}\cdot\delta_{BC}} (\gamma_C^\nabla)^* + \gamma_B^\Delta e^{i\mathbf{k}\cdot\delta_{BC}} (\gamma_C^\Delta)^* \\ e^{i\mathbf{k}\cdot\delta_{AC}} \gamma_C^\nabla (\gamma_A^\nabla)^* + e^{-i\mathbf{k}\cdot\delta_{AC}} \gamma_C^\Delta (\gamma_A^\Delta)^* & e^{i\mathbf{k}\cdot\delta_{BC}} \gamma_C^\nabla (\gamma_B^\nabla)^* + e^{-i\mathbf{k}\cdot\delta_{BC}} \gamma_C^\Delta (\gamma_B^\Delta)^* & |\gamma_C^\nabla|^2 + |\gamma_C^\Delta|^2 \end{pmatrix} \quad (\text{S6})$$

with the site and triangle dependent couplings $\gamma_i^{\Delta/\nabla}$ which can generically be complex, the momentum \mathbf{k} and the difference vectors in the unit cell, $\delta_{\mathbf{x}\mathbf{y}} = \mathbf{r}_x - \mathbf{r}_y$

Since the expressions for complex couplings and gen-

eral \mathbf{k} get rather unwieldy, we present them for real couplings only below.

The zero-mode at generic \mathbf{k} is given by

$$\left\{ e^{-\frac{i}{4}(k_1 + \sqrt{3}k_2)} \left(\gamma_B^\Delta \gamma_C^\nabla e^{\frac{i}{2}\sqrt{3}k_2} - \gamma_C^\Delta \gamma_B^\nabla e^{\frac{ik_2}{2}i} \right), e^{-\frac{i}{4}(k_1 + \sqrt{3}k_2)} \gamma_C^\Delta \gamma_A^\nabla - \gamma_A^\Delta \gamma_C^\nabla e^{\frac{i}{4}(k_1 + \sqrt{3}k_2)}, \gamma_A^\Delta \gamma_B^\nabla e^{ik_1/2} - e^{-\frac{ik_1}{2}} \gamma_B^\Delta \gamma_A^\nabla \right\} \quad (\text{S7})$$

which explicitly shows that both models have a flat band at $E = 0$.

These account for $N_s/3$ of the zero-modes. The remaining missing zero-mode for the MCM is found at $\mathbf{k} = 0$ where the dispersive band touches the flat band

which we discuss next.

Computing the eigenvalues at $\mathbf{k} = 0$ allows us to see how the gap opens for the BDM and remains closed for the MCM. These are given by 0 and

$$\frac{1}{2} \left(\Delta \pm \sqrt{\Delta^2 - 4\gamma_C^{\nabla 2} (\gamma_A^{\Delta 2} + \gamma_B^{\Delta 2}) - 4\gamma_B^{\nabla 2} (\gamma_A^{\Delta 2} + \gamma_C^{\Delta 2}) - 4\gamma_A^{\nabla 2} (\gamma_B^{\Delta 2} + \gamma_C^{\Delta 2}) + 8\gamma_C^\Delta \gamma_C^\nabla (\gamma_A^\Delta \gamma_A^\nabla + \gamma_B^\Delta \gamma_B^\nabla) + 8\gamma_A^\Delta \gamma_B^\Delta \gamma_A^\nabla \gamma_B^\nabla} \right) \quad (\text{S8})$$

with $\Delta = \gamma_A^{\Delta 2} + \gamma_A^{\nabla 2} + \gamma_B^{\Delta 2} + \gamma_B^{\nabla 2} + \gamma_C^{\Delta 2} + \gamma_C^{\nabla 2}$.

This manifestly shows that for the MCM where $\gamma^\Delta = \gamma^\nabla$ the second eigenvalue is also zero corresponding to the band-touching point.

Further, for the BDM where lattice-inversion symmetry is broken, a gap is seen to open up. Eq. (S8) reduces to the expressions given in the main text for the corresponding choices of couplings.

S3. DISORDERED MODELS

Here we provide some additional details on the structure of the flat band states in the disordered models which are not immediately apparent from our explicit construction of all states.

A. Structure of flat band states

We next turn to analyse the structure of the new flat band states in the disordered model.

To this end we consider the total weight of the dispersive states of the clean model in the disordered flat

band

$$\langle \text{FB} | \text{NFB}_0 \rangle = \sum_{\psi_0 \in \text{NFB}} \frac{1}{N_{\text{FB}}} \sum_{\psi \in \text{FB}} |\langle \psi | \psi_0 \rangle|^2 \quad (\text{S9})$$

and the corresponding state resolved-quantity, e.g. the projection of the disordered flat band states ψ onto the dispersive states of the clean model ψ_0 averaged over the flat band

$$\frac{1}{N_{\text{FB}}} \sum_{\psi \in \text{FB}} |\langle \psi | \psi_0 \rangle|^2. \quad (\text{S10})$$

The total weights and the state/energy resolved results for the MCM and BDM are shown in the top and bottom of Fig. S2 respectively. For both models we observe the same scaling $\langle \text{FB} | \text{NFB}_0 \rangle \sim \delta^2$ for the total weights.

However, the state/energy resolved weights differ qualitatively between BDM and MCM. The BDM disordered flat band contains dominantly low-energy states of the clean model and the squared amplitudes decay as a powerlaw $\sim 1/E$ with increasing energy. In contrast, the MCM disordered flat band contains states of all energies of the clean model with equal amplitudes independent of energy.

This can be traced to the fact that the matrixelements $\langle \text{FB} | \mathcal{H} | \psi(E) \rangle$ scale as $E^{1/2}$ and E^1 for BDM and MCM respectively, which when combined with the expected E^{-1} scaling in second order perturbation theory explains the observed behaviour.

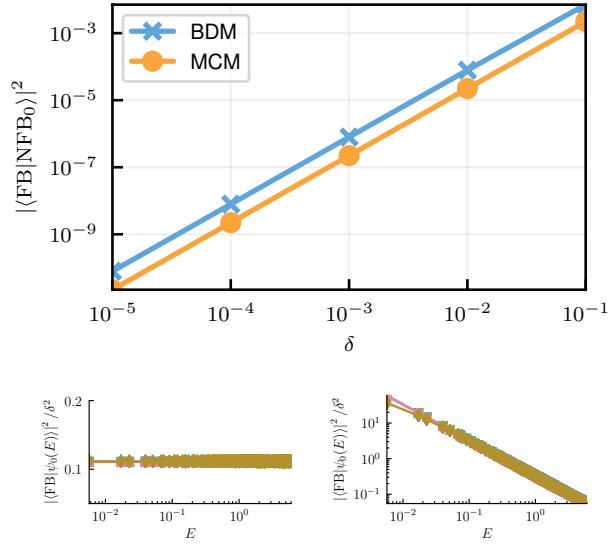


FIG. S2. Top: Total weight of the dispersive states of the clean model of the flat band of the disordered model for MCM (circles) and BDM (x's) Bottom: Energy resolved weight of the dispersive states in the flat band states of the disordered model for MCM (left) and BDM (right), for $\delta = 10^{-5}, 10^{-4}, 10^{-3}, 10^{-2}, 10^{-1}$ (squares, circles, x's, triangles, diamonds) normalised by the observed scaling $\sim \delta^2$. Note that the BDM is on a log-log scale and the MCM on a linear-log scale.